Topological radical pairs produce ultrahigh conductance in long molecular wires

Liang Li[‡1], Shayan Louie[‡1], Austin M. Evans[1], Elena Meirzadeh[1], Colin Nuckolls[*1], and Latha Venkataraman[*1,2]

[1]Department of Chemistry, Columbia University, New York, New York 10027, United States

[2]Department of Applied Physics and Applied Mathematics, Columbia University, New York, New York 10027, United States

ABSTRACT: Molecular one-dimensional topological insulators (1D TIs), which conduct through energetically low-lying topological edge states can be extremely highly conducting and exhibit a reversed conductance decay, affording them great potential as building blocks for nano-electronic devices. However, these properties can only be observed at the short length limit. To extend the length at which these anomalous effects can be observed, we design topological oligo[*n*]emeraldine wires using short 1D TIs as building blocks. As the wire length increases, the number of topological states increases, enabling an increased electronic transmission along the wire, Specifically, we show that we can drive over a microampere current through a single ~5 nm molecular wire, appreciably more than what has been observed in other long wires reported to date. Calculations and experiments show that the longest oligo[7]emeraldine with doped topological states, has an over 10^6 enhancement in the transmission compared to its pristine form. The discovery of these highly conductive, long organic wires overcomes a fundamental hurdle to implementing molecules in complex, nanoscale circuitry: their structures become too insulating at lengths that are useful in designing nanoscale circuits.

INTRODUCTION

Electron transmission through metal-molecule-metal junctions can be engineered by manipulating the chemical structure of the molecular backbone[1, 2] to create nanoscale circuits elements that include insulators,[3] switches,[4, 5] diodes,[6-8] and most commonly, conducting wires.[9] Since the electronic transmission through these devices is ballistic, large currents can be driven across single molecules efficiently without losing energy or electronic phase information. Transport through molecular wires in a coherent and off-resonant regime however leads to an exponential decay of conductance with increasing wire length with[10, 11]

$$G = Ae^{-\beta n} \quad (\beta > 0) \qquad (1)$$

where G is the molecular conductance, A is the pre-exponential coefficient, β is the exponential decay factor, and n is the number of repeating units. To achieve high conductances in long wires, researchers have typically designed wires with conjugated building blocks to achieve a small β, minimizing the decay.[9, 12-15] However, the negative exponential dependence inherent to these wires has left the preparation of long, high conducting wires an unrealized goal.

Over the past decades, electron transport through the topological boundary state of solid-state topological materials has been extensively studied.[16-19] However, studies on electron transmission through topological states at single-molecule level are limited. Solid-state topological insulators (TIs) feature conducting boundary states but insulating interior states. In a molecular TIs, the boundary states, commonly represented by radicals, are at the two ends of the wire. Therefore, the conducting boundary states are called edge states. Conductance across single molecule TIs is dominated by the edge-derived frontier molecular orbitals. The edge states, which are energetically close to the lead Fermi energy, delocalization along the wire backbone and the extent to which the two are coupled dictates the ability to drive current through these states.

It was recently shown that one-dimensional Su-Schrieffer-Heeger-type topological insulators (1D SSH TIs)[20, 21] could yield wires where conductance increases with increasing molecular length. The topological radical states have a finite delocalization length analogous to solitons.[22-24] Taking the prototypical polyacetylene system as an example (Figure 1A, top), at the short chain limit, the two edge states in its diradical resonant structure (red and blue clouds in Figure 1B, top) couple at the center of the chain to generate highly conducting pathways, in which a reversed conductance decay[25-28] ($\beta < 0$) can be obtained. However, at the long chain limit, the two edge states decouple, yielding an exponential decay in conductance due to destructive quantum interference between the two edge-

state derived orbitals.[29] Experimentally, these ideas have been demonstrated in poly-*p*-phenylene wires with radical cations at the edges.[30] However, the experiments showed that a reversed conductance decay is not maintained in these systems beyond ~1.4 nm.

Here, we demonstrate a new strategy to achieve high tunneling current through long wires using a series of 1D TIs as repeating units. This design strategy relies on the electron transport properties in a single 1D SSH TI, where the two radical edge states are spatially close and electronically coupled. To illustrate this concept, we consider a hypothetical polyacetylene wire with radicals on every third carbon (Figure 1B, middle). We use a tight-binding approach to show that the transmission through such a wire does not decay with length in contrast to the polyacetylene terminated with two radicals (Figure 1C, and see Tight-binding analysis section in Supporting Information). Energetically, such a multi-radical polyacetylene is not stable as it would convert to polyene by rearranging its single and double bonds. However, we can modify the backbone structure chemically to stabilize such a wire by replacing all the double bonds with phenylene units and the carbon radicals with nitrogens. In this design, the aromaticity of the phenylenes and the lower on-site energy nitrogen units help to stabilize the radicals. These modifications yield the oligo[*n*]emeraldine (**OE**[*n*]) backbone (Figure 1A, bottom), which can be converted to a multi-radical form t-**OE**[*n*] (topological **OE**[*n*]) through oxidation as shown for the *n*=6 wire in Figure 1B. The edge states of each TI unit are paired and thus for wires with an odd *n*, a single secondary amine is left over (see Figure S1 for t-**OE**[7]).

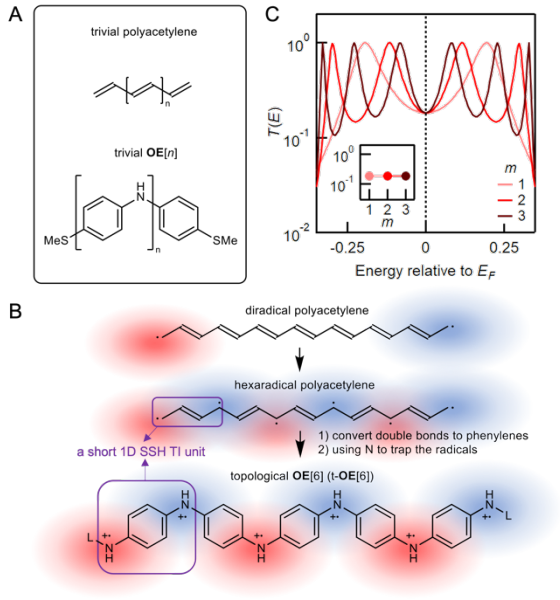

Figure 1. (A) Scheme showing the two molecular backbones, polyacetylene and oligo[n]emeraldine (**OE**[*n*]), shown in their trivial states (i.e. without topological radical states). (B) Structures of a diradical polyacetylene chain (top), a hypothetical hexa-radical polyacetylene chain (middle), and t-**OE**[6] (bottom), red and blue region shows the topological spin states with opposite signs, also indicative of their delocalization ranges. The purple boxes indicate one 1D SSH TI unit of the middle and bottom structures. (C) Calculated transmission functions versus energy for the prototypical multi-radical polyacetylene molecules with m 1D SSH TI units (the middle structure of Figure 1B), the inset figure shows the transmission at Fermi energy (E_F) versus *m*.

RESULTS AND DISCUSSION

We synthesized these wires and then probed their conductance trends using a scanning tunneling microscope-based break junction (STM-BJ) technique,[1, 31] as detailed in the Supporting Information. For the synthesis, the Boc-protected **OE**[*n*] series with n = 2-7 was prepared through a convergent S_NAr, Boc-protection, hydrogenation route followed by a palladium-catalyzed Buchwald-Hartwig coupling to install terminal aurophilic thiomethyl groups (Figure 2A).[32, 33] Thermolytic Boc-deprotection was performed by heating the as-obtained solids at 150 °C for 9 h under vacuum, which yielded pure trivial **OE**[*n*] powders (see Supporting Information for single-crystal X-ray diffraction data, UV-Vis spectra, and cyclic voltammograms). For the STM-BJ measurements, we prepared 0.1 mM solutions of the **OE**[*n*] series in propylene carbonate (PC) with trifluoroacetic acid (TFA). We then oxidize the molecules *in situ* by applying a positive bias to the tip during the STM-BJ measurements.[8] In the presence of TFA, we oxidize **OE**[*n*] to t-**OE**[*n*] that is decorated with radical amine cations, while without TFA, we generate the imine-linked **OE**[*n*] (see Figure S2 for the structure, and see Figure S3-4 for the conductance measurements). Figure 2B shows the 1D conductance histograms for t-**OE**[*n*] with *n* ranging from 2 to 7, measured at an applied bias of +500 mV. The conductance peak for t-**OE**[6] and t-**OE**[7] is above $10^{-2}G_0$ which is significant considering the molecular backbone length of almost 5 nm.

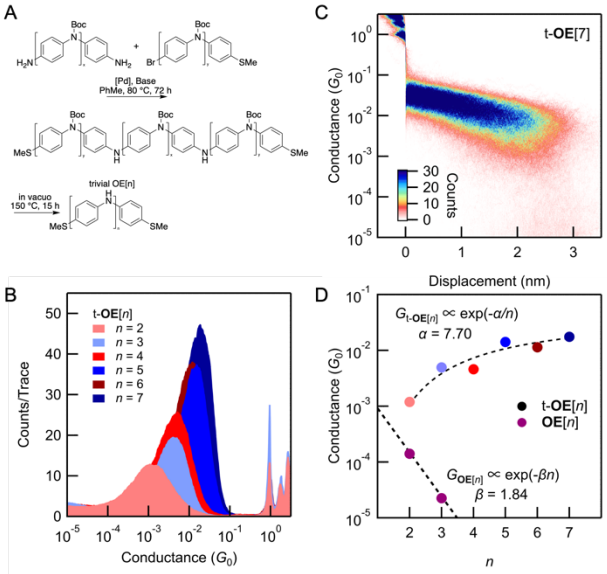

Figure 2. (A) Synthetic route for **OE**[*n*] series. (B) 1D conductance histograms for the t-**OE**[*n*] chains. In the experiment with t-**OE**[*n*] solutions, the charge states are t-**OE**[2] and t-**OE**[3]: 2+; t-**OE**[4] and t-**OE**[5]: 4+; t-**OE**[6] and t-**OE**[7]: 6+. The counter ion is trifluoroacetate (1-). (C) 2D conductance-displacement histogram of t-**OE**[7]. Note that length of the feature in this 2D histogram is shorter than the molecular length because a gap is opened instantly after the rupture of the Au point-contact[35]. (D) The measured conductance of the t-**OE**[n] chains against *n*, showing an attenuated reversed conductance decay trend with fit α = 7.70.

The measured conductance for trivial **OE**[2] and **OE**[3] chains (purple) is also added to this graph, showing a decrease from **OE**[2] to **OE**[3]. Assuming the exponential conductance decay, the fit β = 1.84. For all the molecules, 2000 traces were measured without data selection.

To confirm that we are measuring conductance through molecules containing radicals under these experimental conditions, we measured *ex-situ* electron paramagnetic resonance (EPR) spectra for the t-**OE**[*n*] oxidized with O_2 in the presence of TFA (see Supporting Information), which reveal clear paramagnetic resonance signals consistent with radical-decorated emeraldine polymers.[34] The positive charges in t-**OE**[*n*] planarize the molecular backbone to give a single narrow molecular conductance peak, which is evidenced in the 2D conductance-displacement histogram shown for t-**OE**[7] (Figure 2C, and Figure S3 for other t-**OE**[*n*]).

For the **OE**[*n*] series without radicals, what is referred to as its trivial form, (Figure S6-7), we find that the conductance is clearly distinguishable from the instrument noise floor only for **OE**[2] and **OE**[3] as the conductance decreases with increasing length. Assuming the trivial **OE**[*n*] series fits the exponential conductance decay as described by equation (1), we obtain β = 1.84, in stark contrast to the t-**OE**[*n*]. Furthermore, this would indicate that **OE**[7] would have a conductance of $1.4\times10^{-8}G_0$, a factor of ~1.25 million lower than t-**OE**[7].

To understand the trends in conductance for the t-**OE**[*n*] series, we fit the peaks in the 1D histograms with a Gaussian function and determine the most probable molecular conductance values. In Figure 2D we plot these conductance values against *n*. We observe a clear odd-even effect, likely because we have one neutral amine left in each of the t-**OE**[*n*] wires if *n* is odd (Figure 1). As is clear from these data, the conductance of these molecules increases with increasing molecular length. The conductance does not increase exponentially as the trend is not linear on this semi-logarithm plot. In general, an exponential increase or decrease applies only for wires with a single pair of radicals, i.e., with two topological edge states.[29] However, in t-**OE**[*n*], the number of topological states is not constant but increasing with increasing number of units. Therefore, the hybridization of the increasing topological states near Fermi energy (E_F) leads to distinct evolution of HOMO and LUMO resonances compared to simple 1D TIs, thus the conductance-length regime could be different. We find that our data can be fit by a power law as:

$$G = A'e^{-\alpha/n} \quad (\alpha > 0) \qquad (2)$$

where A' is the pre-exponential coefficient, and the attenuation factor α is 7.70. From equation (2), the attenuated reversed conductance decay indicates that the change in conductance decreases with larger *n*. However, the reversed conductance decay phenomenon still persists, which confirms that we have successfully pushed the length limit of the reversed conductance decay beyond what has been observed previously. For the model in Figure 1C, we get no change in conductance with length, different from what we obtain in the experiment, which is due to the limitation of tight-binding analysis as a single particle approach.

To investigate the robustness of the molecule junction formed by **OE**[*n*], we carried out repeated current-voltage (I-V) sweeps over a range from -1 V to 1 V while holding the longest **OE**[7] molecule (see Supporting Information and Figure 3A, upper panel). We select traces from our measurements that sustain a molecular junction during this entire cycle (~ 50% of the measured traces) and construct a 2D absolute current versus time histogram (Figure 3A. lower panel). This 2D histogram shows that we can maintain **OE**[7] in the molecular junction for a period of 1 second at room temperature. The current exhibits very robust and reproducible feature in every cycle. The current at 1 V reaches a remarkable 4 μA through the t-**OE**[7], distinct from the current in the negative bias region. Note that the current in the negative bias range between 0 and -1 V during ramp down, and -1 V and +0.2 V during ramp up is due to Faradaic and capacitive currents through PC solvent. In Figure 3B we show the I-V characteristics for **OE**[7] from -1 to 1 V within a single cycle of Figure 3A. From -1 to -0.75 V, the current measured is through a neutral **OE**[7] single-molecule junction. From -0.75 to 0.2 V, the current from neutral **OE**[7] is lower than the capacitive current due to the ions in solution. The oxidation processes of **OE**[7] happens between 0.2 V and 0.45 V. Above 0.45 V, the molecule is in its fully oxidized state and a high current is measured. Importantly, these data show that **OE**[7] can be repeatedly reduced and oxidized *in-situ* switching between its topological and trivial forms.

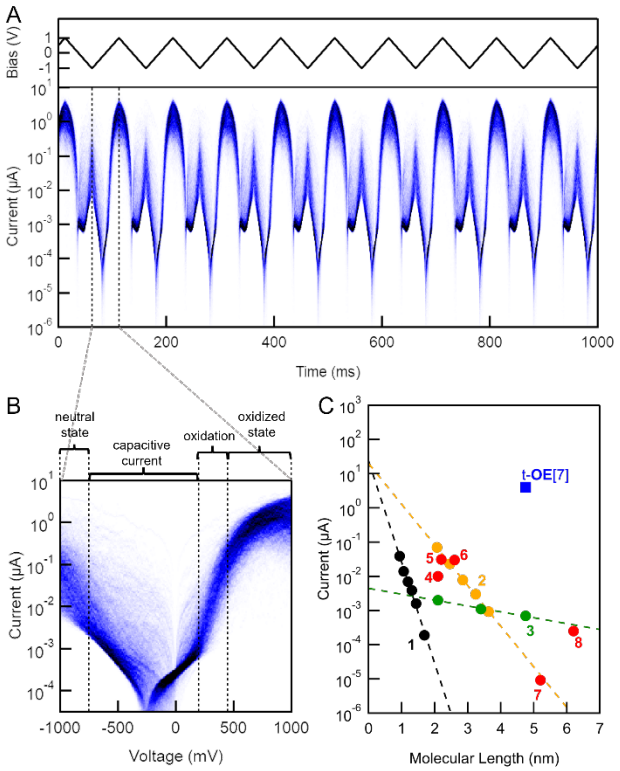

Figure 3. (A) 10-cyclic I-V measurement of t-**OE**[7] chain. Top: bias applied across the junction with a 97 kΩ resistor in series while tip-substrate gap is held constant. Bottom: 2D current–time histogram constructed from a selection of 1,072 from 2,100 traces. (B) I-V curve of t-**OE**[7] from -1 to 1 V obtained from (A). (C) Experimental current through single-molecule junction against molecular length at 1 V bias determined from published works[15,36-42] (see structures in Figure S8). The blue square on the top right shows the current for t-**OE**[7] determined from the I-V sweep shown in Figure 3A.

We next compare the experimental current measured at +1 V through t-**OE**[7] to that of other published[15, 36-42] molecular wires in Figure 3C (see structures in Figure S8). All the current data are obtained at a 1 V. Among the experimental results, t-**OE**[7] is the only molecule that has a current above the microampere level and is at least a 1,000-fold larger than other molecular wires that have similar length. Moreover, because the conductance of longer wires with the same backbone should be close to or higher than that of t-**OE**[7], we could expect even higher current. These results demonstrate how concepts from physical organic chemistry can be applied to achieve record ballistic currents in single-molecule devices. These results also solve a fundamental hurdle that hampers the implementation of molecules in complex circuitry: molecular wires cannot be made sufficiently long enough while maintaining high enough electrical conductivity to be useful.

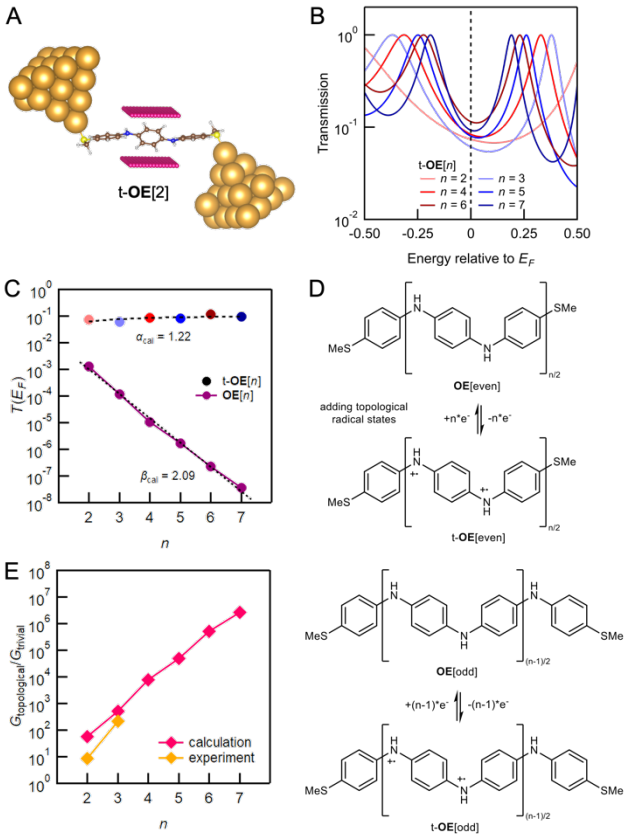

Figure 4. (A) The geometry of t-**OE**[2] in a molecular junction relaxed by DFT, two point-charge squares (pink) are added to constraint the charges on the molecule. (B) Calculated transmission functions of t-**OE**[*n*]. (C) Transmission at E_F against *n* for even (red) and odd (blue) topological chains, both showing reversed conductance decay. Transmission at E_F against *n* for trivial chains is also added to the graph as comparison, showing an exponential decay in conductance. (D) Schemes of doping topological radical states in trivial **OE**[*n*] chains. (E) The comparison between calculations (pink) and experiments (yellow) on the enhancement of conductance upon doping topological states, $G_{topological}/G_{trivial}$, against *n*.

To elucidate the high conductance of topological **OE**[*n*] in the experiments, we calculated the transmission functions of molecular junctions formed with topological **OE**[*n*] using density functional theory (DFT) with non-equilibrium Green's function (NEGF) method using the FHI-aims package[43-45] (see Supporting Information). We first optimize the geometry of the molecule and then attach it to two Au_{22} tetrahedral clusters. In the experiments, the molecules, which are charged, are stabilized by the solvent molecules and the counter ions in the solution which form a delocalization shell of compensating background charges.[30] To emulate the counter charges, we append two square planes of points charges above and below the molecular region to constraint the correct formal charge to the molecule (see Figure 4A, Figure S9, and Table S1). We adjust the magnitude of the point charges by ensuring that the nodal pattern of isolated t-**OE**[*n*] HOMO and LUMO match those of the junction (Figure S10-11). Since the edge states of a 1D SSH TI satisfies spin symmetry, that is, the total number of spins is even, and the number of spin-ups is the same as the number of spin-downs. Hence, the DFT-based calculations are closed-shell.

With these optimizations, we calculate the transmission functions, $T(E)$, for t-**OE**[*n*] (n = 2-7) and plot these against energy relative to E_F in Figure 4B, showing an odd-even dependence. With spin-symmetry of 1D SSH TIs, the spin-up and spin-down channels contribute equally to the total conductances of the molecules. The HOMO and LUMO resonances are quite close to E_F and get closer as *n* increases, which is different from the trend of HOMO-LUMO gap for the isolated topological **OE**[*n*] (Table S2). By contrast, the HOMO and LUMO resonances for the neutral molecule (trivial **OE**[*n*]) are far from E_F (Figure S12), and the DFT calculation of isolated trivial **OE**[*n*] also reveals large HOMO-LUMO gap (Table S3 and Figure S13). The transmission at E_F for t-**OE**[*n*] and trivial **OE**[*n*] are shown in Figure 4C against *n*. For the t-**OE**[*n*], an attenuated reversed conductance decay is confirmed, with α_{cal} = 1.22. The calculated α is affected by the conductance of short chains that are high due to known errors in DFT-based transmission calculations[46]. The DFT transmission calculation also leads to an increased conductance with length instead of the flat trend in Figure 1C. This would also support that this difference is because of the limitations of tight-binding approach. For trivial **OE**[*n*], we also obtain an exponential conductance decay with β_{cal} = 2.09 in approximate agreement with the experiment. For completeness of this study, the transmission of imine-linked **OE**[*n*] series was also calculated (Table S4, Figure S14-16), in line with the experiment.

The consistency of conductance-length trends between the calculations and the experiment confirms ballistic transport through the molecules, i.e., the electrons are tunneling across the molecular orbitals that are formed from a linear combination of the coupled edge states. The tunneling electrons are not changing the redox state of the molecule in the conductance measurements. Once the potential is increased beyond the threshold for oxidation (for example, 0.45 V in Figure 3B for **OE**[7]), the charge state changes and conductance continues across the oxidized molecule through a ballistic mechanism, as we have shown in our earlier work[30].

The DFT calculation results of the topological and trivial series enables us to investigate the relative enhancement of conductance upon doping molecular wires as shown in Figure 4D. In Figure 4E, we show the conductance ratio between the t-**OE**[*n*] and its corresponding trivial **OE**[*n*], $G_{topological}/G_{trivial}$.

Because the transmission ratio of the t-**OE**[*n*] to the trivial **OE**[*n*] increases significantly with wire length, we obtain a transmission enhancement that is a remarkable 2.6 million for **OE**[7]. We also add the experimental data of **OE**[2] and **OE**[3] to Figure 4E, which are in agreement with the data from calculation.

CONCLUSION

Our experimental and theoretical results reveal a reliable method to create highly conducting molecular wires starting with the oligomeric **OE**[*n*] series. By connecting single 1D SSH TI units in series, we overcome the primary shortcoming of molecules created with a single TI unit and show that we can achieve a reversed conductance decay at the long chain limit. For the as-synthesized t-**OE**[*n*] series, we find that the conductance-length relation follows an attenuated reversed conductance decay (equation (2)), which has never been reported before for other trivial closed-shell molecular series. This attenuated reversed conductance decay is the key to making long and highly conducting wires. In principle, there is no theoretical upper limit to the number of 1D SSH TI repeat units that could be embedded within a single chain and as such it is reasonable to expect that for longer analogs of t-**OE**[*n*] ($n > 7$) higher currents and conductances will be achieved.

ASSOCIATED CONTENT

Supporting Information. Additional synthetic, experimental and theoretical methods. This material is available free of charge via the Internet at http://pubs.acs.org.

AUTHOR INFORMATION

Corresponding Authors

Colin Nuckolls – Department of Chemistry, Columbia University, New York, New York 10027, United States; orcid.org/0000-0002-0384-5493; Email: cn37@columbia.edu

Latha Venkataraman − Department of Applied Physics and Applied Mathematics, and Department of Chemistry, Columbia University, New York, New York 10027, United States; orcid.org/0000-0002-6957-6089; Email: lv2117@columbia.edu

Authors

Liang Li – Department of Chemistry, Columbia University, New York, New York 10027, United States; orcid.org/0000-0003-3890-7276.

Shayan Louie – Department of Chemistry, Columbia University, New York, New York 10027, United States.

Austin Evans – Department of Chemistry, Columbia University, New York, New York 10027, United States; orcid.org/0000-0002-3597-2454.

Elena Meirzadeh – Department of Chemistry, Columbia University, New York, New York 10027, United States.

Author Contributions

L. L. and S. L. contributed equally.

Notes

The authors declare no competing financial interest.

ACKNOWLEDGMENT

This research was supported in part by the National Science Foundation under award NSF DMR-1807580. The synthesis was supported by the National Science Foundation under award CHE-2204008 and the U.S. Office of Naval Research under award N00014-20-1-2477. The Columbia University Shared Materials Characterization Laboratory was used extensively for this research. C.N. thanks Sheldon and Dorothea Buckler for their generous support. A.M.E. was supported by the Schmidt Science Fellows, in partnership with the Rhodes Trust. S.L. was supported by the National Science Foundation Graduate Research Fellowship. L.L. thanks Dr. Boyuan Zhang for helpful discussions on DFT transmission calculations.

REFERENCES

(1) Xu, B.; Tao, N. J., Measurement of Single-Molecule Resistance by Repeated Formation of Molecular Junctions. *Science* **2003**, *301*, 1221-1223.

(2) Salomon, A.; Cahen, D.; Lindsay, S.; Tomfohr, J.; Engelkes, V. B.; Frisbie, C. D., Comparison of Electronic Transport Measurements on Organic Molecules. *Adv. Mater.* **2003**, *15*, 1881-1890.

(3) Garner, M. H.; Li, H.; Chen, Y.; Su, T. A.; Shangguan, Z.; Paley, D. W.; Liu, T.; Ng, F.; Li, H.; Xiao, S., Comprehensive Suppression of Single-Molecule Conductance Using Destructive σ-Interference. *Nature* **2018**, *558*, 415-419.

(4) Jia, C.; Migliore, A.; Xin, N.; Huang, S.; Wang, J.; Yang, Q.; Wang, S.; Chen, H.; Wang, D.; Feng, B.; Liu, Z.; Zhang, G.; Qu, D.-H.; Tian, H.; Ratner, M. a.; Xu, H. Q.; Nitzan, A.; Guo, X., Covalently Bonded Single-Molecule Junctions with Stable and Reversible Photoswitched Conductivity. *Science* **2016**, *352*, 1443-1445.

(5) Liljeroth, P.; Repp, J.; Meyer, G., Current-Induced Hydrogen Tautomerization and Conductance Switching of Naphthalocyanine Molecules. *Science* **2007**, *317*, 1203-1206.

(6) Elbing, M.; Ochs, R.; Koentopp, M.; Fischer, M.; von Hanisch, C.; Weigend, F.; Evers, F.; Weber, H. B.; Mayor, M., A Single-Molecule Diode. *Proc. Natl. Acad. Sci. U. S. A.* **2005**, *102*, 8815-8820.

(7) Diez-Perez, I.; Hihath, J.; Lee, Y.; Yu, L.; Adamska, L.; Kozhushner, M. A.; Oleynik, I.; Tao, N., Rectification and Stability of a Single Molecular Diode with Controlled Orientation. *Nat. Chem.* **2009**, *1*, 635-641.

(8) Capozzi, B.; Xia, J.; Adak, O.; Dell, E. J.; Liu, Z.-F.; Taylor, J. C.; Neaton, J. B.; Campos, L. M.; Venkataraman, L., Single-Molecule Diodes with High Rectification Ratios through Environmental Control. *Nat. Nanotechol.* **2015**, *10*, 522-527.

(9) Choi, S. H.; Kim, B.; Frisbie, C. D., Electrical Resistance of Long Conjugated Molecular Wires. *Science* **2008**, *320*, 1482-1486.

(10) Reimers, J.; Hush, N., Analytic Solutions to Resonant and Non-Resonant through-Bridge Electronic Coupling. *Nanotechnology* **1996**, *7*, 417.

(11) Nitzan, A., Electron Transmission through Molecules and Molecular Interfaces. *Annu. Rev. Phys. Chem.* **2001**, *52*, 681-750.

(12) Davis, W. B.; Svec, W. A.; Ratner, M. A.; Wasielewski, M. R., Molecular-Wire Behaviour in p-Phenylenevinylene Oligomers. *Nature* **1998**, *396*, 60-63.

(13) Nitzan, A.; Ratner, M. A., Electron Transport in Molecular Wire Junctions. *Science* **2003**, *300*, 1384-1389.

(14) Lafferentz, L.; Ample, F.; Yu, H.; Hecht, S.; Joachim, C.; Grill, L., Conductance of a Single Conjugated Polymer as a Continuous Function of Its Length. *Science* **2009**, *323*, 1193-1197.

(15) Sedghi, G.; García-Suárez, V. M.; Esdaile, L. J.; Anderson, H. L.; Lambert, C. J.; Martín, S.; Bethell, D.; Higgins, S. J.; Elliott, M.; Bennett, N., Long-Range Electron Tunnelling in Oligo-Porphyrin Molecular Wires. *Nat. Nanotechol.* **2011**, *6*, 517-523.

(16) Zhang, K.-H.; Wang, Z.-C.; Zheng, Q.-R.; Su, G., Gate-Voltage Controlled Electronic Transport through a Ferromagnet/Normal/Ferromagnet Junction on the Surface of a Topological Insulator. *Phys. Rev. B* **2012**, *86*, 174416.

(17) Li, Q.; Rossi, E.; Das Sarma, S., Two-Dimensional Electronic Transport on the Surface of Three-Dimensional Topological Insulators. *Phys. Rev. B* **2012**, *86*, 235443.

(18) Bauer, S.; Bobisch, C. A., Nanoscale Electron Transport at the Surface of a Topological Insulator. *Nat. Commun.* **2016**, *7*, 11381.
(19) Mangnus, M. J. J.; Fischer, F. R.; Crommie, M. F.; Swart, I.; Jacobse, P. H., Charge Transport in Topological Graphene Nanoribbons and Nanoribbon Heterostructures. *Phys. Rev. B* **2022**, *105*, 115424.
(20) Su, W. P.; Schrieffer, J. R.; Heeger, A. J., Solitons in Polyacetylene. *Phys. Rev. Lett.* **1979**, *42*, 1698-1701.
(21) Heeger, A. J.; Kivelson, S.; Schrieffer, J.; Su, W.-P., Solitons in Conducting Polymers. *Rev. Mod. Phys.* **1988**, *60*, 781.
(22) Meier, E. J.; An, F. A.; Gadway, B., Observation of the Topological Soliton State in the Su–Schrieffer–Heeger Model. *Nat. Commun.* **2016**, *7*, 1-6.
(23) Hernangómez-Pérez, D.; Gunasekaran, S.; Venkataraman, L.; Evers, F., Solitonics with Polyacetylenes. *Nano Lett.* **2020**, *20*, 2615-2619.
(24) Wang, S.; Sun, Q.; Gröning, O.; Widmer, R.; Pignedoli, C. A.; Cai, L.; Yu, X.; Yuan, B.; Li, C.; Ju, H.; Zhu, J.; Ruffieux, P.; Fasel, R.; Xu, W., On-Surface Synthesis and Characterization of Individual Polyacetylene Chains. *Nat. Chem.* **2019**, *11*, 924-930.
(25) Zhou, Y. X.; Jiang, F.; Chen, H.; Note, R.; Mizuseki, H.; Kawazoe, Y., Quantum Length Dependence of Conductance in Oligomers: First-Principles Calculations. *Phys. Rev. B* **2007**, *75*, 245407.
(26) Zang, Y.; Fu, T.; Zou, Q.; Ng, F.; Li, H.; Steigerwald, M. L.; Nuckolls, C.; Venkataraman, L., Cumulene Wires Display Increasing Conductance with Increasing Length. *Nano Lett.* **2020**, *20*, 8415-8419.
(27) Leary, E.; Limburg, B.; Alanazy, A.; Sangtarash, S.; Grace, I.; Swada, K.; Esdaile, L. J.; Noori, M.; González, M. T.; Rubio-Bollinger, G., Bias-Driven Conductance Increase with Length in Porphyrin Tapes. *J. Am. Chem. Soc.* **2018**, *140*, 12877-12883.
(28) Ramos-Berdullas, N.; Gil-Guerrero, S.; Peña-Gallego, Á.; Mandado, M., The Effect of Spin Polarization on the Electron Transport of Molecular Wires with Diradical Character. *Phys. Chem. Chem. Phys.* **2021**, *23*, 4777-4783.
(29) Li, L.; Gunasekaran, S.; Wei, Y.; Nuckolls, C.; Venkataraman, L., Reversed Conductance Decay of 1D Topological Insulators by Tight-Binding Analysis. *J. Phys. Chem. Lett.* **2022**, *13*, 9703-9710.
(30) Li, L.; Low, J. Z.; Wilhelm, J.; Liao, G.; Gunasekaran, S.; Prindle, C. R.; Starr, R. L.; Golze, D.; Nuckolls, C.; Steigerwald, M. L.; Evers, F.; Campos, L. M.; Yin, X.; Venkataraman, L., Highly Conducting Single-Molecule Topological Insulators Based on Mono-and Di-Radical Cations. *Nat. Chem.* **2022**, *14*, 1061-1067.
(31) Venkataraman, L.; Klare, J. E.; Tam, I. W.; Nuckolls, C.; Hybertsen, M. S.; Steigerwald, M. L., Single-Molecule Circuits with Well-Defined Molecular Conductance. *Nano Lett.* **2006**, *6*, 458-462.
(32) Singer, R. A.; Sadighi, J. P.; Buchwald, S. L., A General Synthesis of End-Functionalized Oligoanilines via Palladium-Catalyzed Amination. *J. Am. Chem. Soc.* **1998**, *120*, 213-214.
(33) Eelkema, R.; Anderson, H. L., Synthesis of End-Functionalized Polyanilines. *Macromolecules* **2008**, *41*, 9930-9933.
(34) Ji, X.; Xie, H.; Zhu, C.; Zou, Y.; Mu, A. U.; Al-Hashimi, M.; Dunbar, K. R.; Fang, L., Pauli Paramagnetism of Stable Analogues of Pernigraniline Salt Featuring Ladder-Type Constitution. *J. Am. Chem. Soc.* **2019**, *142*, 641-648.
(35) Fu, T.; Frommer, K.; Nuckolls, C.; Venkataraman, L., Single-Molecule Junction Formation in Break-Junction Measurements. *J. Phys. Chem. Lett.* **2021**, *12*, 10802-10807.
(36) Greenwald, J. E.; Cameron, J.; Findlay, N. J.; Fu, T.; Gunasekaran, S.; Skabara, P. J.; Venkataraman, L., Highly Nonlinear Transport across Single-Molecule Junctions via Destructive Quantum Interference. *Nat. Nanotechol.* **2021**, *16*, 313-317.
(37) Fung, E.-D.; Gelbwaser, D.; Taylor, J.; Low, J.; Xia, J.; Davydenko, I.; Campos, L. M.; Marder, S.; Peskin, U.; Venkataraman, L., Breaking Down Resonance: Nonlinear Transport and the Breakdown of Coherent Tunneling Models in Single Molecule Junctions. *Nano Lett.* **2019**, *19*, 2555-2561.
(38) Zang, Y.; Pinkard, A.; Liu, Z.-F.; Neaton, J. B.; Steigerwald, M. L.; Roy, X.; Venkataraman, L., Electronically Transparent Au–N Bonds for Molecular Junctions. *J. Am. Chem. Soc.* **2017**, *139*, 14845-14848.
(39) Low, J. Z.; Capozzi, B.; Cui, J.; Wei, S.; Venkataraman, L.; Campos, L. M., Tuning the Polarity of Charge Carriers Using Electron Deficient Thiophenes. *Chem. Sci.* **2017**, *8*, 3254-3259.
(40) Hines, T.; Diez-Perez, I.; Hihath, J.; Liu, H.; Wang, Z.-S.; Zhao, J.; Zhou, G.; Müllen, K.; Tao, N., Transition from Tunneling to Hopping in Single Molecular Junctions by Measuring Length and Temperature Dependence. *J. Am. Chem. Soc.* **2010**, *132*, 11658-11664.
(41) Inkpen, M. S.; Liu, Z. F.; Li, H.; Campos, L. M.; Neaton, J. B.; Venkataraman, L., Non-Chemisorbed Gold–Sulfur Binding Prevails in Self-Assembled Monolayers. *Nat. Chem.* **2019**, *11*, 351-358.
(42) Meisner, J. S.; Kamenetska, M.; Krikorian, M.; Steigerwald, M. L.; Venkataraman, L.; Nuckolls, C., A Single-Molecule Potentiometer. *Nano Lett.* **2011**, *11*, 1575-1579.
(43) Blum, V.; Gehrke, R.; Hanke, F.; Havu, P.; Havu, V.; Ren, X.; Reuter, K.; Scheffler, M., Ab Initio Molecular Simulations with Numeric Atom-Centered Orbitals. *Comput. Phys. Commun.* **2009**, *180*, 2175-2196.
(44) Arnold, A.; Weigend, F.; Evers, F., Quantum Chemistry Calculations for Molecules Coupled to Reservoirs: Formalism, Implementation, and Application to Benzenedithiol. *J. Chem. Phys.* **2007**, *126*, 174101.
(45) Bagrets, A., Spin-Polarized Electron Transport across Metal–Organic Molecules: A Density Functional Theory Approach. *J. Chem. Theory Comput.* **2013**, *9*, 2801-2815.
(46) Quek, S. Y.; Venkataraman, L.; Choi, H. J.; Louie, S. G.; Hybertsen, M. S.; Neaton, J., Amine−Gold Linked Single-Molecule Circuits: Experiment and Theory. *Nano Lett.* **2007**, *7*, 3477-3482.

TOC Graphics